ISBN: 978-3-95450-227-1 ISSN: 2673-5490 doi:10.18429/JACoW-IPAC2022-WEPOST019

BENCHMARKS OF ENERGY DEPOSITION STUDIES FOR HEAVY-ION COLLIMATION LOSSES AT THE LHC*

J.B. Potoine[1,2], R. Bruce[1], R. Cai[1,3], P. Hermes[1], A. Lechner[1],
S. Redaelli[1], A. Waets[1], Frédéric Wrobel[2]
[1]CERN, Geneva, Switzerland
[2]University of Montpellier, Montpellier, France
[3]École Polytechnique Fédérale de Lausanne, Lausanne, Switzerland

Abstract

During some periods in its second physics run (2015-2018), the LHC has been operated with $^{208}Pb^{82+}$ ion beams at an energy of 6.37 *Z*TeV. The LHC is equipped with a betatron collimation system, which intercepts the transverse beam halo and protects sensitive equipment such as superconducting magnets against beam losses. However, hadronic fragmentation and electromagnetic dissociation of heavy ions in collimators generate off-rigidity particles, which can be lost in the downstream dispersion suppressor, putting the magnets at risk to quench. An accurate modelling of the beam-induced energy deposition in the collimation system and superconducting magnets is important for quantifying possible performance limitations arising from magnet quenches. In this paper, we compare FLUKA shower simulations against beam loss monitor measurements recorded during the 2018 $^{208}Pb^{82+}$ run. In particular, we investigate fast beam loss events, which led to recurring beam aborts in 2018 operation. Based on these studies, we assess the ability of the simulation model to reproduce the observed loss patterns in the collimation and dispersion suppressor region.

INTRODUCTION

Complementing its rich proton physics programme, the Large Hadron Collider (LHC) at CERN also stores and collides fully stripped heavy ion beams ($^{208}Pb^{82+}$) [1]. Heavy-ion operation typically takes place in the last few weeks before the regular winter shutdowns. In the second LHC physics run (2015-2018), a heavy ion energy of 6.37 *Z*TeV and a beam intensity of 1.54×10^{11} Pb ions (733 bunches) was achieved. While the LHC has been designed to store 3.8 MJ per Pb ion beam, it significantly surpassed this value during Run 2 (12.9 MJ) because of the higher-than-nominal intensity [2]. The stored energy is expected to reach an even higher value of 20-20.5 MJ in future runs due to a further increase of the ion energy (6.8-7 *Z*TeV) and beam intensity (2.23×10^{11} Pb ions, 1240 bunches) [2]. In case of beam losses, even a small fraction of the stored beam energy can perturb the LHC performance by leading to superconducting (SC) magnet quenches, a phenomenon during which a SC magnet transits from SC to normal-conducting state due to the heat deposited by particle showers. Therefore, the LHC is equipped with multistage betatron and momentum collimation systems, which are indispensable for protecting the magnets against unavoidable beam halo losses [3].

The collimation systems are organized in well defined hierarchies of more than 100 collimators, which are placed at different transverse positions from the beam. The beam-intercepting components of collimators, called jaws, accommodate blocks most commonly of carbon-fiber composite (CFC), Inermet-180 (tungsten alloy), or MoGR (from 2022) [3, 4]. Each collimator is composed of two jaws. Most of the collimators are located in two insertion regions (IRs), IR7 for betatron cleaning and IR3 for off-momentum cleaning. Operational experience showed that betatron losses dominate over momentum ones. The betatron collimation system exhibits a reduced cleaning efficiency in Pb runs compared to proton runs due to the leakage of secondary fragments to downstream dispersion suppressor (DS) magnets [5]. These secondary ions are the result of hadronic fragmentation and electromagnetic dissociation in collimator blocks, mainly in the primary collimators, which are the first collimators intercepting beam halo particles in the collimation hierarchy. Due to the large dispersion function in the DS, the fragments are lost in distinct lattice cells depending on their magnetic rigidity. Once the Pb ion energy and intensity increases in the future runs, these fragments risk to induce magnet quenches in case the beam lifetime drops to the design value of 0.2 h [4].

Numerical simulations are indispensable for understanding and predicting the power deposition in coils of DS magnets. In order to assess performance limitations and quench margins, an advanced simulation chain has been developed at CERN for studying collimation losses [6, 7]. The simulation chain couples the particle tracking code SixTrack [8, 9] with the Monte Carlo code FLUKA [10–12]. An initial

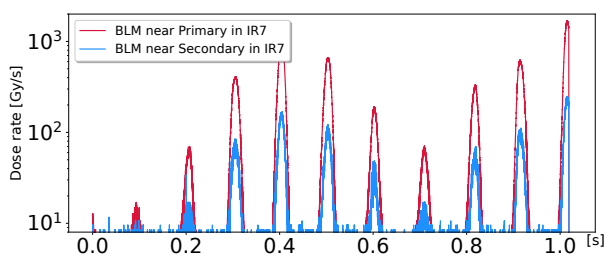

Figure 1: Time profiles of a fast beam loss event measured with BLMs in Run 2 heavy ion operation (28/11/2018). The BLMs were located in the IR7 collimation insertion.

* Research supported by the HL-LHC project.

ISBN: 978-3-95450-227-1 ISSN: 2673-5490 doi:10.18429/JACoW-IPAC2022-WEPOST019

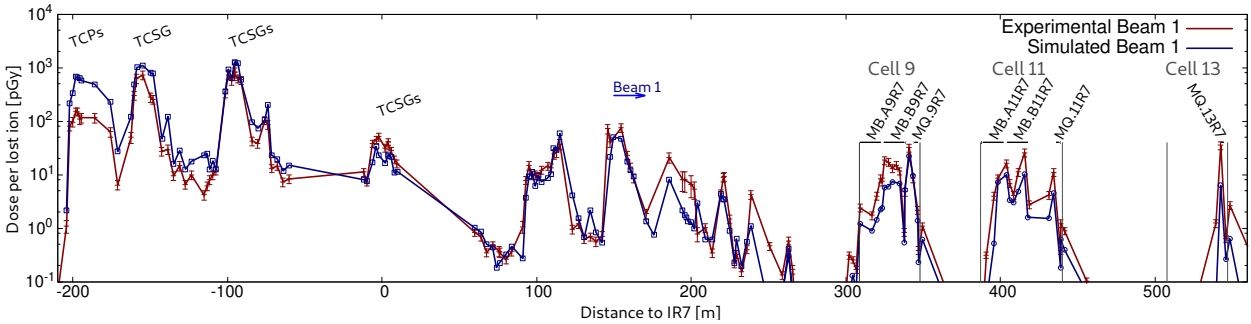

Figure 2: Simulated and experimental BLM signals per Pb ion lost in IR7. The beam direction is from left to right. The labels MQ, MB, TCP and TCSG represent quadrupoles, dipoles, primary and secondary collimators, respectively.

simulation benchmark of the tool for heavy ion collimation losses was carried out in 2015, based on beam loss monitor (BLM) measurements recorded in a controlled beam loss experiment [13, 14]. In this paper, we present a first comparison of simulated BLM signals against measurements from regular heavy ion operation. In particular, we study fast beam loss events, which gave rise to recurring beam aborts in the 2018 heavy ion run (see Fig. 1) [15].

FAST LOSS EVENTS IN RUN 2

Fast beam loss events were recorded during the 2018 heavy ion run, leading to peak loss rates up to a factor of 100 higher than in normal operation [15]. All events occurred on the clockwise rotating beam (Beam 1). The events consisted of multiple loss spikes, which repeated with a 8-12 Hz frequency and exhibited different amplitudes. Each spike lasted about 20-30 ms. Two BLM signals recorded during one of the events (28/11/2018) are shown Fig. 1. In red is a BLM located near the primary collimator, which first intercepts the transverse beam tail. In blue is a BLM located further downstream at a secondary collimator, which intercepts secondary showers and fragments from upstream collimators. The same oscillations could be seen on all BLMs in the IR7 hierarchy of Beam 1. The events exceeded the BLM abort threshold after multiple oscillations, causing a protection dump during 6 out of the 48 planned physics fills [15].

Before any physics run, the betatron cleaning system is qualified by intentionally creating high losses in the horizontal or vertical planes using the transverse damper (so-called loss map). It was observed that the beam loss patterns during the fast loss events observed in operation are qualitatively the same as the beam loss map for horizontal losses around the ring, but with a difference in magnitude. This indicates that the fast loss events generate betatron losses, which were correctly captured by the collimation system.

BENCHMARK OF BLM SIGNALS

In order to benchmark the simulation chain, BLM response simulations were performed for the 2018 machine configuration. In this year, asymmetric settings were used for the right and left jaw of the Beam 1 primary collimator (5σ and 5.5σ, where σ is the transverse beam size as defined in [14]). These asymmetric gaps, which were needed for reducing the leakage to a tertiary collimator, effectively resulted in a one-sided beam cleaning at the horizontal primary collimator. Secondary collimators and active absorbers were positioned at 6.5σ and 10σ (both jaws), respectively. As initial condition, it was assumed that the $^{208}Pb^{82+}$ halo impacts at a certain distance from the edge of the primary collimator's right jaw (horizontal plane). The actual impact parameter is not well known and might vary between loss events. Here a value of 1 μm was assumed, because it leads to the highest fragment leakage to the DS [7, 14]. In Fig. 2, the simulated BLM signals in IR7 and the adjacent cold region (blue curve) are compared to the measured BLM signals (red curve). The measurements were averaged over the different loss events described in the previous section. For each event, the dose values were time-integrated over the loss duration and normalized by the number of ions lost in IR7 during this event. The number of lost ions is the main cause of uncertainty in the study as the losses were close to the achievable resolution of the beam current transformers. The experimental error bars in the figure give the standard deviation of normalized signals from the different loss events. The statistical error of simulation results is a few percent for the highest signals in the IR, but can reach 20% in the DS, which is sufficient for comparing BLM patterns.

An excellent agreement spanning a few orders of magnitude can be observed between simulated and experimental BLM signals. Nevertheless, some discrepancies are found around the primary collimators (around 200 m upstream of IR7) and in the DS (300-450 m downstream of IR7) and the arc (around 560 m). As can be seen in the figure, the simulations overestimate the signals near the primary collimators by about a factor five. In order to assess the possible cause of this overestimation, we investigate the effect of different impact conditions below. In the DS (cells 9 and 11), the simulations are about a factor of two lower than the measurements. A factor 5 underestimation is observed in cell 13 and could be due to the very localized loss location making it very sensitive to any imperfections (e.g. magnet alignment). The different discrepancies found in this study were to some extent also observed in the previous benchmark based on the controlled beam loss test in 2015 [13, 14]. The underestimation in the DS was, however, a factor 2.5 larger in the

ISBN: 978-3-95450-227-1 ISSN: 2673-5490 doi:10.18429/JACoW-IPAC2022-WEPOST019

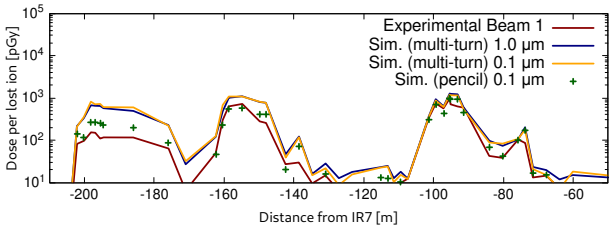

Figure 3: Simulated and measured BLM pattern around the primary and the first secondary collimators. The yellow and blue curves take into account the spread of multi-turn impacts on the primary collimator, whereas the green dots assume that all ions always impact on the same position.

previous study. This can partly be explained by the choice of a larger impact parameter in the previous simulation; tracking studies indicated that an impact parameter larger than 1 μm reduces the leakage to the DS [7, 14]. The present results show that even the worst case impact parameter still leads to an underestimation in the DS. In addition, the previous benchmark was performed for Beam 2, which can be subject to a different leakage than beam 1.

SENSITIVITY TO INITIAL CONDITIONS

In order to probe the sensitivity of BLM signals at the primary collimator to the beam loss conditions, different sub-μm impact parameters were studied. Figure 3 presents BLM patterns around the primary and first secondary collimators, considering impact parameters of 0.1 μm and 1 μm on the primary, respectively. The results show only a little dependence on the initial condition. The reason is that the impacts are smeared out by the multi-turn beam dynamics, considering that not all Pb ions will be subject to an inelastic nuclear collision or to electromagnetic dissociation during the first impacts. As a consequence, the ions can make several turns in the machine and can impact at a larger position with respect to the collimator edge in subsequent turns. A lower initial impact parameter increases the number of turns after their first impact and leads to a more diluted impact distribution. This increases the average impact parameter and therefore the BLM signals are very similar between the different cases.

The figure also shows a non-physical case (green dots), where the spatial spread of multi-turn impacts on the primary collimator is not simulated. Instead, Pb ions surviving the impact and making another turn in the machine were artificially loaded again at their initial position on the primary (0.1 μm from the edge). This study case shows smaller discrepancies of BLM signals near the primaries and the first secondaries, possibly indicating that the multi-turn spread inside the right jaw of the primary collimators is overestimated in the other simulations (blue and yellow lines) .

ISOTOPE LEAKAGE

Figure 4 shows the energy loss map on the DS aperture, identifying the contributions of some of the most abundant

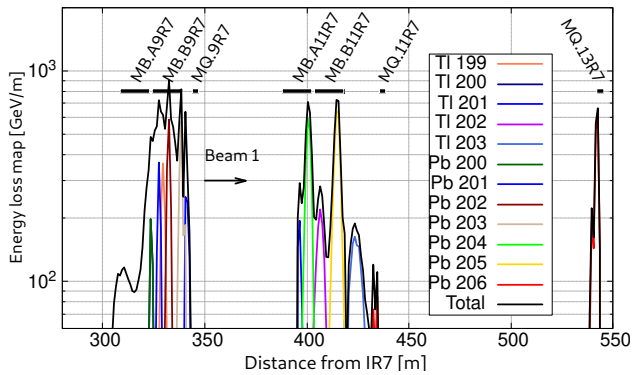

Figure 4: Energy loss map on the DS aperture downstream of the betatron cleaning insertion. The most abundant heavy isotopes are shown.

heavy fragments with a magnetic rigidity allowing them to reach the DS. Those particles are the ones responsible for the subsequent particle showers that produce the BLM signals. The losses in the different cells are dominated by different Pb and Tl isotopes, with a mix of lighter fragments (not shown) in the first loss cluster. The loss position is closely correlated with the magnetic rigidity and therefore the ion species. Heavier isotopes of a given element are lost further downstream. For example, the losses in cell 13 are composed of Pb^{206} ions, while lighter Pb isotopes are lost in cells 9 and 11. Considering the systematic differences between simulated and measured BLM signals, the energy loss map suggests that the underestimation of measurements in the DS is not due to a single isotope species, but can likely be attributed to multiple ones. In one of the most exposed magnets (MB.B9R7 in Fig. 4), both light and heavy fragments are possibly underestimated. This would indicate that the discrepancy between simulation and measurements is probably not due to individual isotope production yields in collimators. As observed in proton collimation studies [13], the reason for the discrepancies could be a possible underestimation of the leakage in general, probably caused by machine imperfections, which are not accounted for in the simulation.

CONCLUSIONS

Based on fast beam loss events observed in Run 2 operation, this paper presented a benchmark of the SixTrack-FLUKA coupling for heavy ion beam collimation. Taking into account the complexity of ion-matter interactions and fragment production in collimators, the simulation chain yields a satisfying agreement with measurements, which gives confidence in our understanding of operational beam losses. In particular, the simulation reproduces BLM signals in the dispersion suppressor within a factor of two. This is an important finding since the fragment leakage to DS magnets remains the main bottleneck for heavy ion collimation.

ISBN: 978-3-95450-227-1 ISSN: 2673-5490 doi:10.18429/JACoW-IPAC2022-WEPOST019

REFERENCES

[1] J. M. Jowett, "Colliding Heavy Ions in the LHC," in *Proc. IPAC'18*, Vancouver, Canada, Apr.-May 2018, pp. 584–589, doi:10.18429/JACoW-IPAC2018-TUXGBD2

[2] R. Bruce, M. Jebramcik, J. Jowett, T. Mertens, and M. Schaumann, "Performance and luminosity models for heavy-ion operation at the CERN Large Hadron Collider," *Eur. Phys. J. Plus*, no. 745, 2021, doi:https://doi.org/10.1140/epjp/s13360-021-01685-5

[3] R. W. Assmann *et al.*, "The Final Collimation System for the LHC," in *Proc. EPAC'06*, Edinburgh, UK, Jun. 2006, paper TUODFI01, pp. 986–988.

[4] O. Aberle *et al.*, *High-Luminosity Large Hadron Collider (HL-LHC): Technical design report*. CERN, Geneva, Switzerland, 2020, doi:10.23731/CYRM-2020-0010

[5] P. Hermes *et al.*, "Measured and simulated heavy-ion beam loss patterns at the CERN Large Hadron Collider," *Nucl. Instrum. Methods Phys. Res. A*, vol. 819, pp. 73–83, 2016, doi:http://dx.doi.org/10.1016/j.nima.2016.02.050

[6] E. Skordis *et al.*, "FLUKA coupling to Sixtrack," in *Proc. the ICFA Mini-Workshop on Tracking for Collimation, Geneva, Switzerland, 30 October 2018*, vol. 2/2018, 2018, pp. 17–25.

[7] P. D. Hermes, "Heavy-Ion Collimation at the Large Hadron Collider: Simulations and Measurements," PhD-thesis, Westfälische Wilhelms-Universität Münster and CERN, 2016.

[8] F. Schmidt, "SIXTRACK, users reference manual," CERN, Tech. Rep. Report No. SL/94-56 (AP), 1994.

[9] G. Robert-Demolaize, R. W. Assmann, S. Redaelli, and F. Schmidt, "A New Version of SixTrack with Collimation and Aperture Interface," in *Proc. PAC'05*, Knoxville, TN, USA, May 2005, paper FPAT081, pp. 4084–4086.

[10] G. Battistoni *et al.*, "Overview of the FLUKA code," *Annals of Nuclear Energy*, vol. 82, pp. 10–18, 2015, Joint International Conference on Supercomputing in Nuclear Applications and Monte Carlo 2013, SNA + MC 2013., doi:https://doi.org/10.1016/j.anucene.2014.11.007

[11] C. Ahdida *et al.*, "New capabilities of the FLUKA multi-purpose code," *Front. Phys.*, vol. 9, 2022, doi:https://doi.org/10.3389/fphy.2021.788253

[12] *FLUKA.CERN website*, https://fluka.cern/.

[13] E. Skordis *et al.*, "Study of the 2015 Top Energy LHC Collimation Quench Tests Through an Advanced Simulation Chain," in *Proc. IPAC'17*, Copenhagen, Denmark, May 2017, pp. 100–103, doi:10.18429/JACoW-IPAC2017-MOPAB012

[14] N. Fuster-Martinez *et al.*, "Simulations of heavy-ion halo collimation at the CERN Large Hadron Collider: Benchmark with measurements and cleaning performance evaluation," *Phys. Rev. Accel. Beams*, no. 23, p. 111 002, 2020, doi:10.1103/PhysRevAccelBeams.23.111002

[15] D. Mirarchi, G. Arduini, M. Giovannozzi, A. Lechner, S. Redaelli, and W. J, "Special losses during LHC Run 2," in *Pro. the 9th Evian Workshop on LHC Beam Operation*, Evian Les Bains, France, 2019, pp. 213–220.